The nuclear effective interaction was assumed to be energy-independent and taken to be a δ function. Virtual states with one particle in the continuum were included explicitly. This produced a significant shift down in energy and considerable mixing of the resonance states found in the discrete shell-model calculations. The mixing of analog spin directly by the effective interaction and through the continuum was studied in detail. For a δ-function force, the direct mixing is proportional to the difference between bound proton and neutron states. This was found to be small in most cases. The mixing through the continuum produced significant analog spin mixing. In the 16–17-MeV region two $J^\pi = 1^-$ states exhibited a complete breakdown of analog spin.

The $J^\pi = 1^-$ states in the giant dipole region were given special attention. Due to the effects of the Coulomb force there are three 1^- states in this energy region with significant dipole strength. This implies isospin mixing. However, it was pointed out that this is an example of the dynamic criterion for isospin conservation. The states overlap strongly and contribute coherently to a resultant reaction amplitude which conserves isospin.

The photonuclear cross sections were calculated using a matrix formulation which guarantees unitarity. The magnitude of the cross section was much too large. Part of this discrepancy is clearly due to the fact that the Tamm-Dancoff approximation was employed.[13] Most of the dipole strength was found to lie in the 22-MeV state rather than in both states as found experimentally. This will be discussed in a future paper.

[13] J. D. Perez and G. J. Stephenson, Bull. Am. Phys. Soc. **13**, 1463 (1968).

PHYSICAL REVIEW VOLUME 182, NUMBER 4 20 JUNE 1969

Proton Spin Flip in the Reaction $^{12}C(p, p')^{12}C^*$ [4.44 MeV]*

J. J. KOLATA† AND A. GALONSKY
Cyclotron Laboratory, Michigan State University, East Lansing, Michigan 48823

(Received 14 January 1969)

The angular correlation between protons inelastically scattered from the first excited state of ^{12}C and the subsequent 4.44-MeV deexcitation γ radiation perpendicular to the scattering plane was measured for 26.2- and 40.0-MeV incident proton energy. This correlation has previously been shown to be related to the fraction of protons undergoing spin flip along this direction. As has been observed at lower bombarding energies, the spin-flip probability peaks at large proton scattering angles; observed here are probabilities as high as 0.35 near 150°. The spin-flip probability for all inelastic scattering to the 4.44-MeV state is 3%. The data were compared to the predictions of the distorted-wave Born approximation, using collective-model and microscopic-model form factors. The expected sensitivity to the spin-dependent part of the nucleon-nucleus interaction was confirmed. However, it was found that the observed spin flip was almost entirely accounted for by distortions in the entrance and exit elastic channels, due to the spin-orbit term in the optical-model potential. No definite conclusions regarding the spin-dependent part of the inelastic interaction could be reached from the ^{12}C data, possibly owing to the failure of the assumptions of the optical model for such light nuclei. It appears that meaningful information regarding the spin dependence of the reaction mechanism producing the excited state can be obtained from spin-flip data only for those nuclei having well-determined optical-model parameters.

I. INTRODUCTION

SEVERAL experimental techniques are available for studying the spin dependence of the nucleon-nucleus interaction. In particular, one might investigate the inelastic scattering of polarized protons,[1] or the effects of target polarization on a particular reaction.[2] Either of these methods involves the preparation of an initial system with known spin orientation; the relative scarcity of such data reflects the experimental difficulties encountered. Alternatively, it is possible to determine the angular dependence of polarization of the residual nucleus, when the initial system is completely unpolarized. Usually, one observes the angular correlation involving the scattered particle and the deexcitation γ radiation. It can be shown,[2,3] in the context of the distorted-wave Born approximation (DWBA) with unique total transferred angular momentum, that the information obtained by this method is the same as that obtained by scattering from polarized targets. Therefore, such measurements can provide valuable data concerning the spin dependence of nuclear reaction

* Work supported in part by the National Science Foundation.
† Present address: Naval Research Laboratory, Washington, D.C. 20390.
[1] M. P. Fricke, E. E. Gross, and A. Zucker, Phys. Rev. **163**, 1153 (1967); C. Glashausser, R. DeSwiniarski, and J. Thirion, *ibid.* **164**, 1437 (1967).
[2] L. J. B. Goldfarb and D. A. Bromley, Nucl. Phys. **39**, 408 (1962).
[3] G. R. Satchler, Nucl. Phys. **55**, 1 (1964).

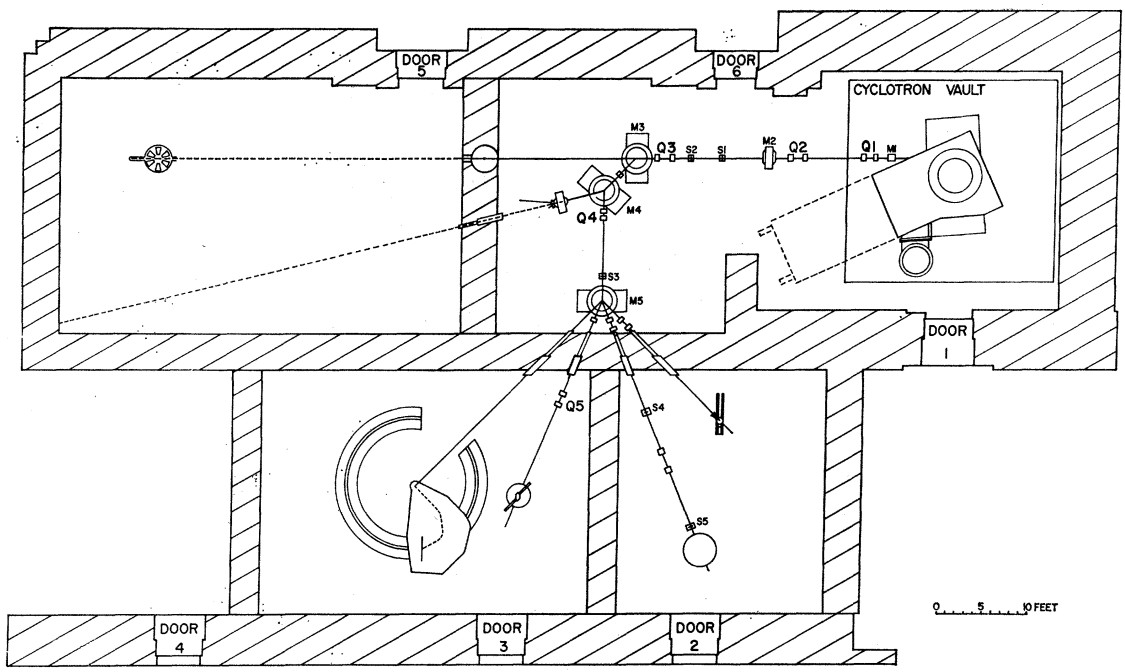

FIG. 1. Scale drawing of the cyclotron and ancillary beam-handling equipment. Q1–Q5 are quadrupole doublets. Energy analysis is accomplished by the bending magnets M3 and M4. S1–S3 are the beam-defining apertures mentioned in the text.

mechanisms for the wide range of nuclei for which polarized targets are unavailable; in addition, they can provide supplementary information in those cases for which inelastic scattering of polarized protons has been measured. The chief disadvantage of the method lies in the need to perform a coincidence experiment.

The angular correlation function for the case in which γ radiation is detected in the plane determined by the incident beam and the scattered particle (in-plane correlation) has been analyzed in the DWBA by several authors.[4,5] Banerjee and Levinson[5] predicted the form

$$W(\theta_\gamma) = A + B \sin^2 2(\theta_\gamma - \epsilon_1) + C \sin^2(\theta_\gamma - \epsilon_2), \quad (1)$$

and associated the last term with the presence of spin flip in the interaction. Such a term has been observed,[6] but it has proved to be very difficult to extract the relevant spin-flip probability, which is expected to be quite sensitive to the spin dependence of the nucleon-nucleus interaction.

Recently, Schmidt *et al.*[7] have pointed out that spin flip could be more easily studied through an angular correlation in which the γ radiation is detected along the normal to the scattering plane (γ-perpendicular correlation). They were able to show that this correlation is directly proportional to the spin-flip probability, in the case of a $0^+ - 2^+$ transition. The argument may be extended with minor modifications to the excitation of a $1^\pm$ or 2^- state from a 0^+ ground state. We have used this method to investigate proton spin flip in the excitation of the first 2^+ state in ^{12}C by 26.2- and 40.0-MeV protons. The data have been analyzed in the DWBA, with several different reaction models, in an attempt to determine the type of information about spin-dependent nucleon-nucleus forces which can be extracted from spin-flip measurements.

In Sec. II, we present a description of the experimental method and the determination of the spin-flip probability. Section III is devoted to the discussion of the DWBA analysis, including the reaction models and optical-model parameters used.

II. EXPERIMENTAL METHOD

A. Beam Line

Figure 1 is a scale drawing of the beam transport system. A proton beam from the Michigan State University Isochronous Cyclotron was focussed by a set of quadrupole doublets on the object slit S1 of an energy analysis system formed by magnets M3 and M4. The properties of this system has been investigated previously,[8] so that we were able to calculate the

[4] G. R. Satchler, Proc. Phys. Soc. (London) **A68**, 1037 (1955); J. S. Blair and L. Wilets, Phys. Rev. **121**, 1493 (1961).
[5] M. K. Banerjee and C. A. Levinson, Ann. Phys. (N.Y.) **2**, 499 (1957).
[6] H. Yoshiki, Phys. Rev. **117**, 773 (1960); T. H. Braid, J. L. Yntema, and B. Zeidman, Argonne National Laboratory Report No. 6358, p. 11 (unpublished).
[7] F. H. Schmidt, R. E. Brown, J. B. Gerhart, and W. A. Kolasinski, Nucl. Phys. **52**, 353 (1964).
[8] G. H. Mackenzie, E. Kashy, M. M. Gordon, and H. G. Blosser, IEEE Trans. Nucl. Sci. **14**, 450 (1967); J. L. Snelgrove and E. Kashy, Nucl. Instr. Methods **52**, 153 (1966).

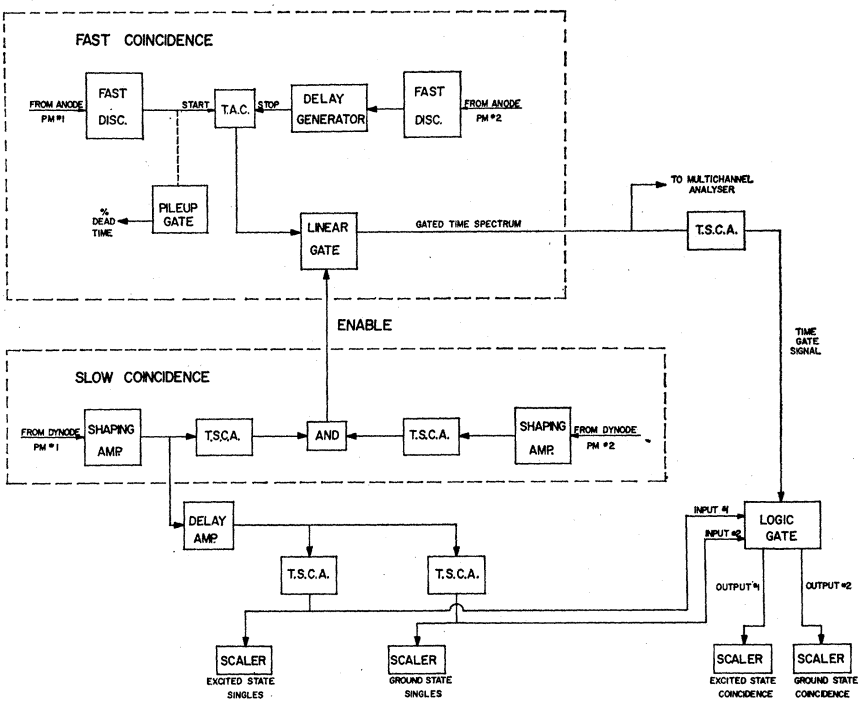

FIG. 2. Block diagram of the electronics. TAC is a time-to-amplitude converter. TSCA is a timing single-channel analyzer, which gives an output when the bipolar-input signal crosses zero.

transmitted beam energy to ± 0.1 MeV. The energy spread in the beam, determined from the slit openings, varied from 25–50 keV full width at half-maximum (FWHM).

The analyzed beam was deflected into the appropriate experimental area by magnet M5, and focused on the target by the final quadrupole doublet Q5. Typical beam spot size was 4 mm wide by 2 mm high, with an angular spread of less than $\pm 0.5°$. No collimating slits were used near the target in an attempt to keep background radiation in the experimental area to a minimum. Instead, the beam was positioned by observing a 0.125-mm-thick plastic scintillator at the target position, using a closed-circuit television system. Fiducial marks were inscribed on the scintillator. In this way, the beam could be centered to within 1 mm. The scintillator was inserted several times during the course of a run to check against centering drifts, which did not occur. After passing through the target, the beam was collected in a 7.5-cm-diam Faraday cup placed 2 m beyond the target position.

The target was a 26.5-mg/cm^2 graphite foil[9]; its uniformity was determined to be better than $\pm 1\%$ by monitoring elastic proton scattering from various areas of the sample. The energy loss ΔE in the target was 495 keV at 26 MeV, and 350 keV at 40 MeV. The mean proton energy E_p was determined by subtracting $\frac{1}{2}\Delta E$ from the energy determined by the beam transport system. The target was contained in a small evacuated chamber with 0.125-mm-thick Mylar windows.

[9] Speer Carbon Co., Inc., Car bon Products Div., St. Marys, Pa.; Shield Grade 9326.

B. Detectors and Electronics

Scattered protons were detected in a 3.8-cm-diam by 1.9-cm-thick NaI(Tl) scintillator mounted on an RCA 8575 photomultiplier. The energy resolution of this system was typically 600-keV FWHM at 24 MeV. Target-to-detector distance was 18–24 cm, and the full angle subtended at the circular collimator was 6°–8°. The detector was mounted on a remotely adjustable arm which could be positioned to $\pm 0.1°$.

Deexcitation γ radiation was detected in a 5-cm-diam by 7.5-cm-long NaI(Tl) scintillator, also mounted on an RCA 8575 photomultiplier. The best energy resolution obtained was 7.5% FWHM for the 662-keV γ ray from ^{137}Cs. This assembly was positioned on the normal to the scattering plane to within 4 mm, and the distance from the beam line to the center of the scintillator was 41 cm, corresponding to an 0.5° angular positioning uncertainty; the scintillator subtended a full angle of 7° at its center. The γ detector was shielded from background radiation by a 130-kg cylindrical Pb shield.

A block diagram of the electronics is shown in Fig. 2. Anode pulses from the photomultipliers were used to start and stop a time-to-amplitude converter (TAC). The time spectrum was gated by the output of a conventional zero-crossing slow coincidence unit with a resolving time (2τ) of 1 μsec. Timing single-channel

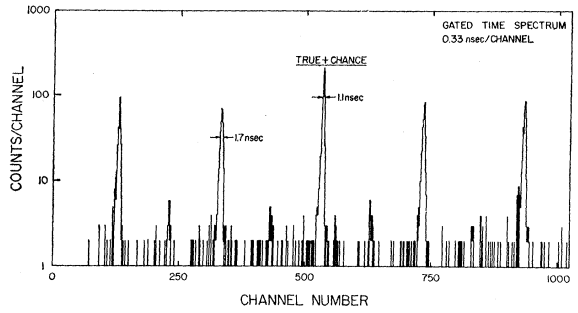

FIG. 3. Gated time spectrum taken at 26 MeV. The indicated resolution is the FWHM of the peak. The "chance" peaks have a somewhat larger width due to the contribution from the burst width of the beam. When the chance peak is subtracted from the "true+chance" events, the resulting "true" peak has a width of 0.9 nsec (FWHM). The small peaks between the main beam bursts are due to the background coming from the Faraday cup, which was located 2 m beyond the target position.

analyzers (TSCA) provided both time and pulse-height information in the slow coincidence channel. In practice, they were used to reduce the number of accidental coincidences due to low-level background pulses in both detectors.

A typical gated time spectrum taken at 26 MeV is shown in Fig. 3. At this energy, the pulse-repetition rate of the beam is 15.1 MHz, so that the separation between beam bursts is 66 nsec. The relative delays have been adjusted so that the peak containing true coincidences occurs near the center of the spectrum. Typical resolution obtained for this peak was 1 nsec (FWHM), and the best value obtained was 0.8 nsec (FWHM). The somewhat larger width of the accidental peaks is due to a contribution from the pulse width of the beam. The small peaks between the main beam bursts correspond to accidental coincidences with background γ radiation coming from the Faraday cup. A window set around the "true+chance" peak in this time spectrum was narrow enough to keep these events, as well as a large fraction of the continuous background between peaks, from contributing to the accidental rate.

The count rate in both detectors was kept below 10^4 counts/sec at the fast discriminator output. Observation of the shaping amplifier outputs, and a measurement of the average time between pulses using a pileup gate, indicated that coincidence losses due to dead time were small at these count rates. The largest dead-time correction made was 14%.

C. Data Reduction

The output of the coincidence circuitry was used to gate both the elastic and inelastic (4.44-MeV) events. Since the elastically scattered protons cannot be in true coincidence with a 4.44-MeV γ ray, these events give a measure of the accidental rate. The number of accidental coincidences N_A was determined from the expression

$$N_A = N_{\mathrm{gsc}}(N_{4.4s}/N_{\mathrm{gss}}), \qquad (2)$$

where N_{gsc} is the number of ground-state coincidences, and N_{gss} ($N_{4.4s}$) is the total number of ground-state (inelastic 4.4-MeV) singles events.

The number of true coincidences at each angle was normalized to the total number of inelastic 4.44-MeV events, and the experimental angular-correlation function was calculated using the equation

$$W(\theta_p) = N(\theta_p)/\epsilon_\gamma\Omega_\gamma, \qquad (3)$$

where $\epsilon_\gamma\Omega_\gamma$ is the product of the efficiency and solid angle of the γ-ray detector, and $N(\theta_p)$ is the normalized number of true coincidences. The product $\epsilon_\gamma\Omega_\gamma$ was measured[10] for each setting of the γ-ray discriminator in the slow coincidence unit, using the method described in Ref. 7. The accuracy of the measurement was $\pm 9\%$ at 26.2 MeV and $\pm 14\%$ at 40.0 MeV.

The spin-flip probability S_1 was determined, apart from a small correction term, from the equation[7]

$$S_1(\theta_p) = (8\pi/5)W(\theta_p). \qquad (4)$$

The correction term mentioned is due to the finite acceptance angle of the two detectors, and its magnitude depends on the details of the population of the various

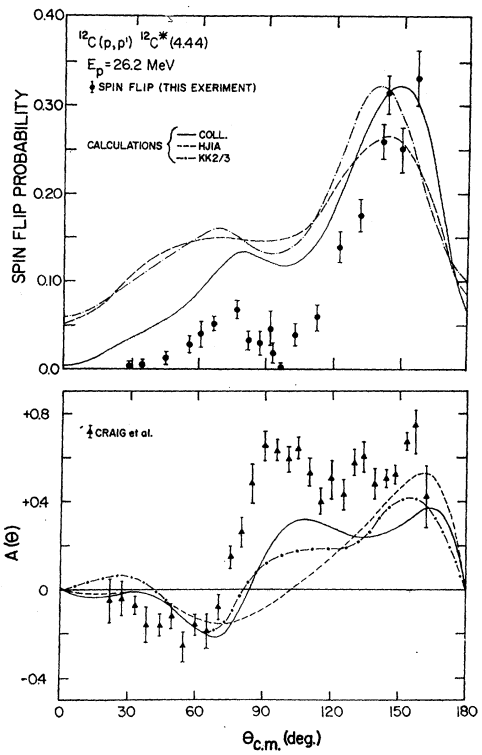

FIG. 4. Spin-flip and inelastic asymmetry at E_p=26.2 MeV. The spin-flip data are from the present experiment; the asymmetry data are taken from Ref. 28. The various curves are the results of DWBA calculations in the collective model (COLL), and in the microscopic model using impulse approximation (HJIA) and Kallio-Kolltveit (KK2/3) form factors.

[10] R. Sager, National Science Foundation Undergraduate Research Participation Program Report, Michigan State University, 1967 (unpublished).

magnetic sublevels of the 2^+ state.[7] However, a maximum and minimum value for the correction term can be determined. For a circular proton (γ ray) detector aperture subtending an angle of $2\epsilon_p$ ($2\epsilon_\gamma$) rad, it can be shown[11] that the maximum and minimum corrections are given to second order by

$$\Delta S_1(\max) = -\tfrac{1}{2}[\epsilon_\gamma^2+\tfrac{1}{2}\epsilon_p^2-\tfrac{1}{32}(\epsilon_p^4/\epsilon_\gamma^2)] \times[3-(44\pi/5)W(\theta_p)]-\tfrac{3}{5}\pi\epsilon_p^2W(\theta_p)-\tfrac{1}{2}(3/2)^{1/2}\epsilon_p^2 \times[1-(8\pi/5)W(\theta_p)], \quad (5)$$

$$\Delta S_1(\min) = -\tfrac{1}{2}[\epsilon_\gamma^2+\tfrac{1}{2}\epsilon_p^2-\tfrac{1}{32}(\epsilon_p^4/\epsilon_\gamma^2)] \times[1-(28\pi/5)W(\theta_p)]+\tfrac{3}{5}\pi\epsilon_p^2W(\theta_p). \quad (6)$$

We have applied a correction equal to the average of these limits, and included in the uncertainty in S_1 a contribution equal to one-half the difference of the limits. Both the correction and its uncertainty were very small, since $\epsilon_p^2=\epsilon_\gamma^2=3.4\times10^{-3}$ for this experiment. As an example, the correction is $(-4.8\pm3.3)\times10^{-3}$ for $S_1=0.100$.

The measured spin-flip probabilities appear in Figs. 4 and 5. The error bars shown correspond to the relative errors only. There is an uncertainty in the absolute spin-flip probability of 9% for the data taken at 26.2 MeV, and 14% for the 40.0-MeV data, owing to the uncertainty in the efficiency of the γ-ray detector.

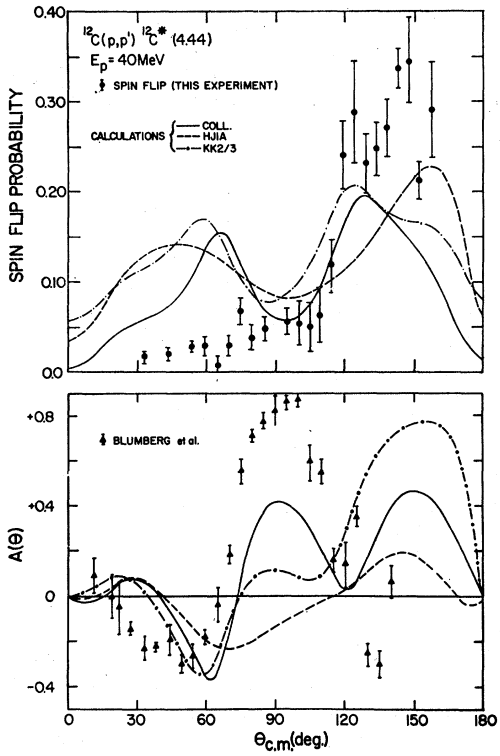

FIG. 5. Spin-flip and inelastic asymmetry at 40 MeV. The spin-flip data are from the present experiment; the asymmetry data are taken from Ref. 27. The various curves are the results of DWBA calculations (see caption, Fig. 4).

III. ANALYSIS

A. Transition Amplitude

In the zero-range DWBA theory of inelastic scattering, the transition amplitude takes the form[3]

$$T_{fi}=\chi_{m_f'm_f}^{(-)*}(r)\langle\psi_f \mid V \mid \psi_i\rangle\chi_{m_i'm_i}^{(+)}(r)\,dr, \quad (7)$$

where m denotes the z component of spin. This expression neglects particle-exchange effects.

The functions χ_i and χ_f are the distorted waves, which are eigenstates of elastic scattering from the target in its initial and final state, respectively. They are usually generated from an optical-model potential using parameters which fit the elastic scattering data. Note that the spin-orbit term present in the optical-model potential can couple different spin projections, so that the distorted waves are, in general, nondiagonal matrices in spin space. The off-diagonal terms ($m\neq m'$) lead to a nonzero spin-flip amplitude.

The remaining factor in the expression (7) for the transition amplitude is the matrix element of the interaction causing the transition, taken between the initial and final states of the target. It contains all of the information about the structure of these states and the mechanism which couples them, and can be looked upon as producing transitions between the elastic scattering eigenstates χ_i and χ_f. Since this matrix element will, in general, be spin-dependent, it can also couple different spin projections and therefore produce a nonzero spin-flip amplitude.

The transition amplitude T_{fi} is usually expanded in terms of reduced amplitudes[3] corresponding to the transfer of a definite total angular momentum $\mathbf{j}$, orbital angular momentum $\mathbf{l}$, and spin angular momentum $\mathbf{s}$ to the nucleus during the inelastic event. These transferred angular momenta are determined from the relationships

$$\mathbf{j}=\mathbf{J}_f-\mathbf{J}_i, \quad \mathbf{s}=\mathbf{S}_i-\mathbf{S}_f, \quad \mathbf{l}=\mathbf{j}-\mathbf{s}, \quad \pi_i\pi_f=(-1)^l, \quad (8)$$

where the transition is $(J^\pi)_i\rightarrow(J^\pi)_f$ and $\mathbf{S}_i$ ($\mathbf{S}_f$) is the spin of the incident (scattered) particle. Note that the value of each of these angular momenta during the inelastic event is to be used. This is not necessarily the same as the asymptotic value. For example, a reduced amplitude labeled by $s=0$ may still contribute to spin flip ($s=1$ asymptotically) through the distortions induced by the spin-orbit term in the optical potential.

B. Reaction Models

The radial part of the nuclear matrix element, or form factor,[3] was calculated using three different reaction models. The first two were microscopic models, in which the nuclear wave functions were taken to be shell-model states, and the effective interaction potential

[11] J. J. Kolata, thesis, Michigan State University, 1969 (unpublished).

V was assumed to be the sum of two-body forces. The third was a collective model, in which the nuclear wave functions were taken to be the eigenstates of **J**, the total angular momentum of the nucleus, and the effective interaction potential was generated from a deformed optical-model potential.

1. Microscopic Models

Assuming that multiple scattering processes are unlikely, the projectile interacts with the target nucleus through an interaction potential of the form[12]

$$V=\sum_i v_{ip}-U, \tag{9}$$

where U is the optical potential used to generate the distorted waves, and v_{ip} is the two-body interaction between the projectile and the ith nucleon in the target. Furthermore, v_{ip} is usually approximated by the expression[12–14]

$$v_{ip}=V_0(|\mathbf{r}_i-\mathbf{r}_p|)+V_i(|\mathbf{r}_i-\mathbf{r}_p|)\boldsymbol{\sigma}_i\cdot\boldsymbol{\sigma}_p, \tag{10}$$

where $\boldsymbol{\sigma}_i$ ($\boldsymbol{\sigma}_p$) is the spin operator for the target (projectile) nucleon. This expression neglects the tensor and spin-orbit forces known to be present in the interaction between free nucleons.[15,16] The main justification for this truncation is simplicity; noncentral two-body forces are much more difficult to work with,[17] and the present state of the theory does not seem to justify using the extra parameters. However, tensor forces have been used to study certain reactions.[18]

We have used two types of radial dependence in the expression (10). The first was of the form

$$V_s(r)=V_s\exp(-\alpha_s r)/\alpha_s r \qquad (s=0,1). \tag{11}$$

The range and strength parameters were obtained[19] in the impulse approximation by fitting the Fourier transform of a single Yukawa to the nucleon-nucleon scattering amplitude calculated from the central part of the Hamada-Johnston potential.[16] The interaction so determined is complex and spin-dependent, and both the range and strength parameters vary with incident proton energy. The second form for the radial dependence of Eq. (10) was derived from the Kallio-Kolltveit shell-model effective interaction.[20] The resulting interaction was real, spin-dependent, and independent of energy. In addition, a factor depending on the two-thirds power of the nucleur matter density, which seems to improve the agreement between theory and experiment,[21] was included. In both cases, the wave functions of Gillet and Vinh Mau[22] were used in the calculation of the form factor.

2. Collective Model

In the collective model, the inelastic interaction is derived from a deformed, nonspherical optical potential, which is expanded in a Taylor series about the mean radius. The interaction is taken to be that part of the expansion which occurs to first order in the deformation parameter.[23] Thus, the shape of the form factor is given by a radial derivative of the optical-model potential.

It has been customary to deform only the real and imaginary central part of the optical potential[23]; more recent studies, however, indicate that the spin-orbit[1,24] terms must also be deformed to account for the observed polarization in inelastic proton scattering. The spin-orbit term is particularly difficult to handle, since the deformed part contains a gradient operator leading to nonradial terms. Calculations have been performed using the full prescription[24,25] and also with a somewhat simplified version of the spin-orbit term[1] which does not contain the gradient operator.

We have calculated collective-model form factors for a deformed complex central potential. Such an interaction is spin-independent and can contribute no $s=1$ amplitude. In this model, then, the entire spin-flip cross section is due to spin-orbit distortions in the elastic channels.

C. Optical-Model Potential

Optical potentials used in the DWBA calculations were determined from an analysis of published elastic cross-section[26–28] and polarization[28–30] data taken at 26.2, 40.0, and 49.5 MeV. We used a local optical potential of the form

$$U(r)=-Vf(x_R)-i(W-4W_D d/dx_I)f(x_I)$$
$$+(\hbar/m_\pi c)^2(V_{so}+iW_{so})\boldsymbol{\sigma}\cdot\mathbf{l}(1/r)(d/dr)f(x_{so}), \tag{12}$$

where $f(x_k)=[\exp(x_k)+1]^{-1}$, $x_k=(r-r_kA^{1/3})/a_k$, to

[12] G. R. Satchler, Nucl. Phys. **A95**, 1 (1967).
[13] A. K. Kerman, H. McManus, and R. M. Thaler, Ann. Phys. (N.Y.) **8**, 551 (1959).
[14] M. B. Johnson, L. W. Owen, and G. R. Satchler, Phys. Rev. **142**, 748 (1966).
[15] K. E. Lassila, M. H. Hull, Jr., H. M. Ruppel, F. A. McDonald, and G. Breit, Phys. Rev. **126**, 881 (1962).
[16] T. Hamada and I. D. Johnston, Nucl Phys. **34**, 383 (1962).
[17] G. R. Satchler, Nucl. Phys. **77**, 481 (1966).
[18] C. Wong, J. D. Anderson, J. McClure, B. Pohl, V. A. Madsen, and F. Schmittroth, Phys. Rev. **160**, 769 (1967).
[19] H. McManus, F. Petrovich, and D. Slanina, Bull. Am. Phys. Soc. **12**, 12 (1967); F. Petrovich, D. Slanina, and H. McManus, Michigan State University Report No. MSPT-103, 1967 (unpublished).
[20] A. Kollio and K. Kolltveit, Nucl. Phys. **53**, 87 (1964).
[21] A. M. Green, Phys. Letters **24B**, 384 (1967); A. Lande and J. P. Svenne, *ibid.* **25B**, 91 (1967).
[22] V. Gillet and N. Vinh Mau, Nucl. Phys. **54**, 321 (1964).
[23] R. H. Bassel, G. R. Satchler, R. M. Drisko, and E. Rost, Phys. Rev. **128**, 2693 (1962).
[24] H. Sherif and J. S. Blair, Phys. Letters **26B**, 489 (1968).
[25] R. O. Ginaven, E. E. Gross, J. J. Malanify, and A. Zucker, Phys. Rev. Letters **21**, 552 (1968).
[26] J. K. Dickens, D. A. Haner, and C. N. Waddell, Phys. Rev. **132**, 2159 (1963).
[27] J. A. Fannon, E. J. Burge, D. A. Smith, and N. K. Ganguly, Nucl. Phys. **A97**, 263 (1967).
[28] L. N. Blumberg, E. E. Gross, A. VanDerWoude, A. Zucker, and R. H. Bassel, Phys. Rev. **147**, 812 (1966).
[29] R. M. Craig, J. C. Dore, G. W. Greenlees, J. Lowe, and D. L. Watson, Nucl. Phys. **79**, 177 (1966).
[30] R. M. Craig, J. C. Dore, G. W. Greenlees, J. Lowe, and D. L. Watson, Nucl. Phys. **83**, 493 (1966).

TABLE I. Optical-model parameters which produced the fits to the ^{12}C elastic data shown in Figs. 6 and 7.[a]

E_P (MeV)	V (MeV)	r_R (F)	a_R (F)	W_D (MeV)	r_I (F)	a_I (F)	V_{so} (MeV)	r_{so} (F)	a_{so} (F)	χ_σ^2/N_σ	χ_P^2/N_P[b]
26.2	48.48	1.07	0.634	3.33	1.34	0.682	7.34	1.01	0.485	22	7
40.0	45.06	1.08	0.689	5.19	1.25	0.533	7.45	1.08	0.485	22	18
49.5[c]	43.36	1.08	0.712	6.61	1.21	0.527	8.16	1.02	0.531	56	6

[a] As mentioned in the text, the final calculations were performed with a surface imaginary form ($W=0.0$) and a real spin-orbit term ($W_{so}=0.0$).

[b] The experimental uncertainties quoted in Refs. 26–30 were used in the computation of χ_σ^2 and χ_p^2. $N_\sigma(N_P)$ is the number of cross-section (polarization) data points.

[c] The data at 49.5 MeV were analyzed to aid in the determination of the energy dependence of the parameters. The fits obtained are not shown.

which is added the Coulomb potential of a uniformly charged sphere of radius $1.20A^{1/3}$ F and charge Ze interacting with a point charge. Here, r_k and a_k are the usual radius and diffuseness parameters of the optical model,[1] and k refers to one of (R, I, so). All calculations were performed with the search code GIBELUMP,[31] which minimizes $\chi_T^2=\chi_\sigma^2+\chi_p^2$ using the standard definition of χ^2.[1] When two sets of parameters gave equivalent χ_T^2, preference was given to the set resulting in smaller χ_p^2.

Preliminary searches were made with volume imaginary ($W_D=0$) and surface imaginary ($W=0$) potentials, and also with a mixture of the two forms. In the latter case, it was found that W and W_D were strongly correlated. That is, the search code tended to drive one or the other of them to zero, depending on initial conditions. This correlation has been previously noted[32] for ^9Be and ^{12}C. For this reason, pure surface imaginary potentials, which seemed to give somewhat better fits than volume types, were used throughout the final analysis. Furthermore, it was found that the optimum value for the imaginary spin-orbit depth W_{so} tended to be very close to zero, in agreement with previous observations[1,32]; it was therefore set equal to zero in the remaining searches. The other 9 parameters were allowed to vary independently; the final values obtained for them appear in Table I. The corresponding fits are shown in Figs. 6 and 7.

The optical-model potentials for the entrance and exit channels in the DWBA calculations were determined from a smooth curve representing the observed energy dependence of the parameters presented in Table I. The resulting values appear in Tables II and III. No attempt was made to include the effects of a possible spin-spin interaction in the exit channel. This type of interaction has been shown to be negligible[33] for nuclei as light as ^{27}Al.

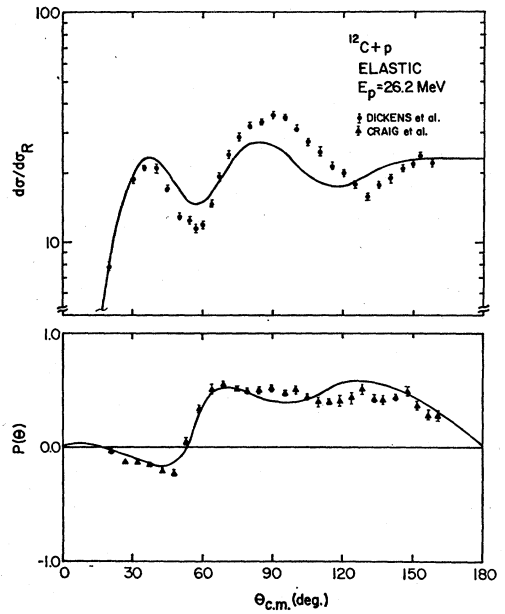

FIG. 6. Optical-model fits to ^{12}C elastic data at $E_p=26.2$ MeV, using the parameters of Table I. The cross-section data are taken from Ref. 25; the polarization data are taken from Ref. 28.

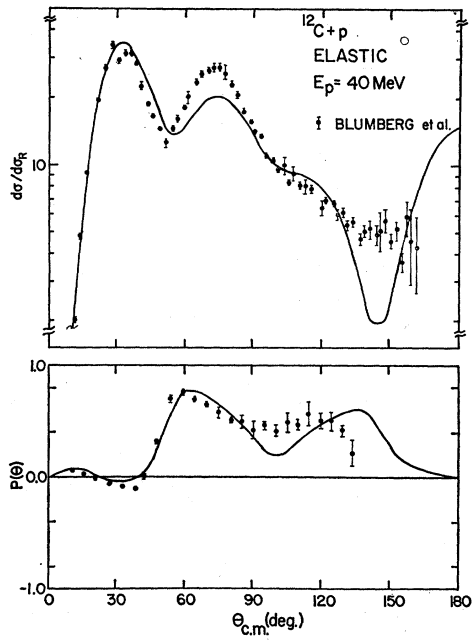

FIG. 7. Optical-model fits to ^{12}C elastic data at $E_p=40$ MeV, using the parameters of Table I. The data are taken from Ref. 27.

[31] FORTRAN-IV optical-model search code written by F. G. Perey and modified for the CDC-3600 by R. M. Haybron at the Oak Ridge National Laboratory.

[32] G. R. Satchler, Nucl. Phys. **A100**, 497 (1967).

[33] L. Rosen, J. E. Brolley, Jr., and L. Stewart, Phys. Rev. **121**, 1423 (1961).

TABLE II. Entrance-channel optical-model parameters used in the DWBA calculations.

E_P (MeV)	V (MeV)	r_R (F)	a_R (F)	W_D (MeV)	r_I (F)	a_I (F)	V_{so} (MeV)[a]	r_{so} (F)	a_{so} (F)
							8.10	1.13	0.555
26.2	48.5	1.07	0.636	3.38	1.34	0.648	7.13	1.04	0.472
							6.30	0.96	0.415
							8.50	1.10	0.550
40.0	45.0	1.08	0.685	5.15	1.26	0.570	7.65	1.04	0.500
							7.00	0.96	0.465

[a] For the spin-orbit parameters, the first (third) number given is the largest (smallest) value the parameter can have such that χ_T^2 is increased by less than 25% from its minimum value. The second number given is the "optimum" value of the parameter.

D. Calculations

The inelastic data have been analyzed in the DWBA,[34] using form factors calculated according to the three models previously described.

1. Differential Cross-Section Predictions

Figure 8 shows the differential cross sections predicted by the collective model ("COLL"), the impulse approximation ("HJIA"), and the Kallio-Kolltveit interaction ("KK2/3"), along with the inelastic scattering data of Refs. 26 and 28. The predictions of the collective model are normalized to the experimental total cross section; the value of the deformation parameter determined from the normalization was 0.66, in agreement with previous results.[32]

The best agreement with the cross-section data was obtained from the collective model, at both 26.2 and 40 MeV. The impulse-approximation calculations are in rather poor agreement with experiment at 26.2 MeV, although the situation improves somewhat at the higher energy. On the other hand, it should be noted that the predictions of the Kallio-Kolltveit interaction are not very different from those of the collective model at either energy. None of the calculations was able to reproduce the small backward peak observed in the 40.0-MeV differential cross section.

2. Asymmetry and Spin-Flip Predictions

The inelastic asymmetries and spin-flip probabilities calculated with the three models are shown in Figs. 4 and 5, along with the experimental data. Both microscopic-model calculations include the contributions of an $s=1$ amplitude arising from the spin-dependent part of the interaction. The collective model in which the spin-orbit part of the optical potential is not deformed does not lead to such an amplitude.

The agreement obtained with the experimental inelastic asymmetry data was at best only qualitative, even in the collective model. The phase predictions of this model are reasonably good at both energies, but the calculated magnitudes are far too small. The impulse-approximation predictions are again quite different from those of the collective model, and are in generally poorer agreement with experiment; the quality of the fits obtained in this model deteriorated at the higher energy, where the cross-section fits, Fig. 8, improved. Finally, it should be noted that the predictions of the Kallio-Kolltveit model again resemble those of the collective model.

TABLE III. Exit-channel optical-model parameters used in the DWBA calculations.

E_P (MeV)	V (MeV)	r_R (F)	a_R (F)	W_D (MeV)	r_I (F)	a_I (F)	V_{so} (MeV)[a]	r_{so} (F)	a_{so} (F)
							8.00	1.13	0.555
26.2	50.0	1.07	0.626	2.77	1.36	0.675	6.98	1.04	0.464
							6.10	0.96	0.400
							8.30	1.15	0.550
40.0	46.0	1.08	0.670	4.65	1.28	0.594	7.46	1.04	0.490
							6.75	0.96	0.450

[a] For the spin-orbit parameters, the first (third) number given is the largest (smallest) value the parameter can have such that χ_T^2 is increased by less than 25% from its minimum value. The second number given is the "optimum" value of the parameter.

[34] The code was written by R. M. Haybron and T. Tamura. The routine to calculate the spin-flip probability was added by one of us (J.K.). All calculations were performed on the SDS $\Sigma-7$ computer at the cyclotron laboratory.

The spin-flip predictions of the three models are in semiquantitative agreement with the experiment data. The largest discrepancies occur at the forward angles, where the spin flip probability is consistently overestimated. The predicted total spin-flip probabilities are much too large, as can be seen from the data presented in Table IV.

It is interesting that the collective model, which contains no $s=1$ amplitude, predicts a spin-flip probability in reasonable agreement with the experimental data. We conclude that the observed spin-flip is almost entirely due to the distortions introduced into the entrance and exit elastic-channel wave functions by the spin-orbit term in the optical potential. This implies

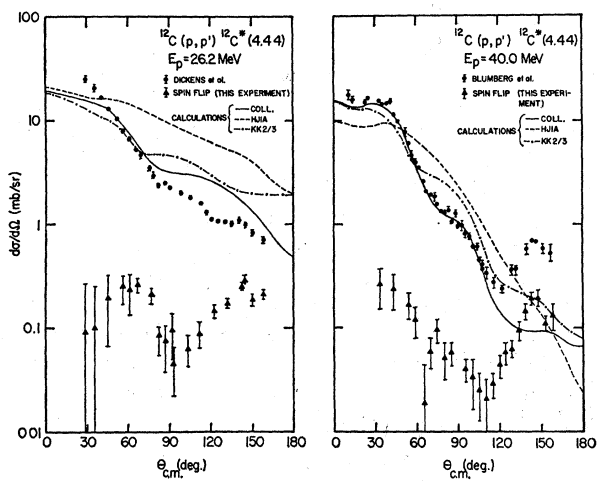

FIG. 8. Inelastic cross-section data for first excited state of ^{12}C, for $E_p=26.2$ and 40 MeV. The 26.2-MeV data are taken from Ref. 25. The 40-MeV data are taken from Ref. 27. The spin-flip cross sections at both energies were determined by multiplying the spin-flip probabilities (see Figs. 4 and 5) by the appropriate differential cross section. The various curves are the results of DWBA calculations (see caption, Fig. 4).

that if any meaningful information regarding the $s=1$ part of the inelastic interaction is to be obtained from spin-flip data, the experiment must be performed for nuclei having very well determined optical-model parameters so that the effects of spin-orbit distortion can be separated from those of the $s=1$ amplitude of the inelastic interaction.

We have performed a series of calculations in which the parameters of the spin-orbit term in the optical potential were varied in an attempt to determine the sensitivity of the spin-flip predictions to these parameters. First, we determined the range over which the parameters could be varied such that χ_T^2 for the fits to the elastic data increased by less than 25%. The limits of the range appear in Tables II and III for each of the parameters. Distorted-wave calculations were then made using the upper or lower limits for one of the parameters, while fixing the remaining parameters at their optimum values. In each case, the form factors given by the impulse approximation were used. The results of these calculations at 26.2 MeV appear in Figs. 9 and 10. It appears that spin-flip predictions are slightly more sensitive to the spin-orbit parameters than are the inelastic asymmetries. In fact, it should be possible to use the spin-flip data to determine the spin-orbit term in the optical potential for those cases in which a polarized beam is unavailable. This has already been done[35] for the scattering of ^3He on ^{12}C. A major difficulty is that it is not practical to program an automatic search routine for DWBA calculations.

TABLE IV. Total spin-flip probability.

E_p (MeV)	Experiment	Theory (COLL)	Theory (HJIA)	Theory (KK2/3)
26.2	0.0275±0.0055	0.0875	0.1480	0.1420
40.0	0.0325±0.0075	0.0720	0.1190	0.1190

In the same spirit, a number of calculations was performed in an attempt to determine the effect of the $s=1$ amplitude on the predictions of the microscopic

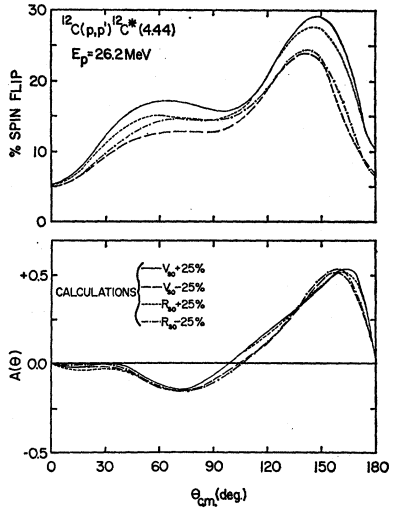

FIG. 9. Distorted-wave Born-approximation calculations for spin-flip and inelastic asymmetry in the reaction $^{12}C(p, p')^{12}C^*$ [4.44] at $E_p=26.2$ MeV. The various curves correspond to different spin-orbit parameters in the optical-model potentials, as described in the text. The notation $V_{so}+25\%$, for example, means that the spin-orbit depth used was the largest value which gave less than 25% increase in χ_T^2 over its minimum value in the optical-model analysis. Similarly, $R_{so}-25\%$ means that the spin-orbit radius used was the smallest value which gave less than 25% increase in χ_T^2. The corresponding values for V_{so} and R_{so} in the entrance and exit channels appear in Tables II and III. All other parameters were fixed at their optimum values. The form factor used in all calculations was that given by the impulse approximation.

[35] D. M. Patterson and J. G. Cramer, Phys. Letters **27B**, 373 (1968).

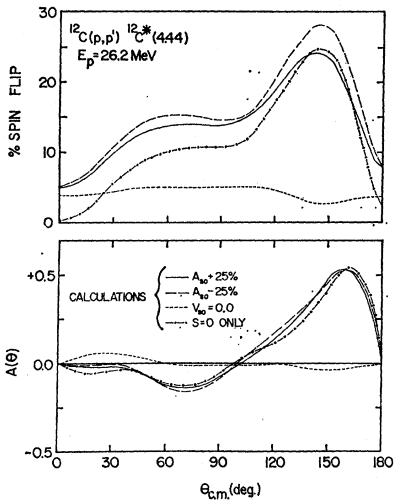

FIG. 10. Distorted-wave Born-approximation calculations for spin-flip and inelastic asymmetry in the reaction $^{12}C(p, p')^{12}C^*$ [4.44] at E_p=26.2 MeV. The notation (A_{so}±25%) is explained in the caption to Fig. 9. The calculation with V_{so}=0.0 gives an indication of the spin flip and asymmetry due to the s=1 part of the inelastic interaction. The calculation with S=0 only shows the contribution to the spin flip and asymmetry due to spin-orbit distortions in the elastic channel wave functions. The form factor given by the impulse approximation was used for all these calculations.

model, again using impulse approximation form factors. Two types of calculations were performed. In the first case, the optimum optical-model parameters of Tables II and III were used, but the s=1 amplitude was set equal to zero. In the second type of calculation, the s=1 amplitude was that predicted by the impulse approximation, and the spin-orbit term in the optical potential was set equal to zero. The results of these calculations at 26.2 MeV also appear in Fig. 10. It is clear that the s=1 amplitude has a negligible effect on the asymmetries, and only a small effect on the spin-flip predictions. The predicted spin-flip probability is increased by an amount which is almost independent of angle, so that the greatest differences occur at the forward angles, where the spin flip is smallest.

IV. CONCLUSIONS

The spin-flip probability for protons inelastically scattered from the first excited state of ^{12}C has been measured for incident proton energies of 26.2 and 40.0 MeV. The data exhibit large backward peaks similar to those observed at lower energies[7] and for other nuclei.[24] Comparison with DWBA calculations indicates that semiquantitative fits to the experimental data can be obtained with collective-model and microscopic-model form factors. The predictions display a marked sensitivity to the spin-orbit term in the optical potential, and are only slightly affected by the presence of an s=1 amplitude in the microscopic-model form factors.

No definite conclusions regarding the spin-dependent part of the inelastic interaction can be obtained from the present data. In fact, the addition of an s=1 amplitude to the microscopic form factors seemed to make the agreement with experiment worse in that it significantly increased the predicted spin flip at the forward angles, where it was already too large. However, in view of the inability of any of the models to reproduce the inelastic assymmetries, and considering the fact that optical-model parameters which adequately fit all of the elastic data could not be found, it would seen that the difficulty lies in the failure of the assumptions of the optical model for nuclei as light as ^{12}C. If this is the case, then accurate spin-flip measurements for heavier nuclei having well determined optical-model parameters may give useful information regarding the spin dependence of the inelastic reaction mechanism.

ACKNOWLEDGMENTS

The authors would like to thank R. Sager for his help in the collection of the data and the measurement of the γ detector efficiency. In addition, we would like to acknowledge the help of Dr. B. Preedom in the optical-model analysis. The microscopic-model form factor programs and the impulse-approximation calculations were due to F. Petrovich. We are indebted to Dr. R. Haybron for supplying the DWBA code, and to Dr. P. Locard and Dr. S. Austin for their helpful comments on the DWBA calculations.